



Publication Year	2017
Acceptance in OA	2021-02-02T15:28:27Z
Title	Properties of a Local Dust Storm on Atlantis Chaos, Mars
Authors	Oliva, Fabrizio, Geminale, A., ALTIERI, FRANCESCA, BELLUCCI, Giancarlo, CARROZZO, FILIPPO GIACOMO, D'Aversa, E., Sindoni, G., GRASSI, Davide
Handle	http://hdl.handle.net/20.500.12386/30171

PROPERTIES OF A LOCAL DUST STORM ON ATLANTIS CHAOS, MARS.

F. Oliva, (*fabrizio.oliva@iaps.inaf.it*), A. Geminale, F. Altieri, G. Bellucci, F.G. Carrozzo, E. D'Aversa, G. Sindoni, D. Grassi, *Istituto di Astrofisica e Planetologia Spaziali, Rome, Italy.*

Introduction:

The study of suspended dust on Mars is fundamental to understand the planet's thermal structure and climate (Kahre et al., 2008). Martian aerosols are mainly composed of micron-sized particles, probably produced by soil weathering (Korablev et al., 2005). A permanent dust haze is always present in the atmosphere and is characterized by an opacity of about 0.05 - 0.2 at 9.3 μm . The actual dust loading varies with circulation, season and geographic region and in presence of dust storms its opacity may increase significantly reaching several units (Altieri et al., 2007).

The radiative effects of dust depend on the size, the composition and the optical properties of its particles (Maattanen et al., 2009). In the visible-near infrared (VIS-NIR) spectral range they have a low single scattering albedo and contribute to the heating of the lower atmosphere whereas in the infrared (IR) they efficiently radiate heat to space through IR emission (Korablev et al., 2005).

Global dust storms are believed to be caused by a positive feedback between the dust content and the intensity of the atmospheric motion (Gierasch and Goody, 1968). In this study we present the analysis of the dust properties in a local storm imaged in the Atlantis Chaos region by the OMEGA spectrometer (Bibring et al., 2004) on March 2nd 2005 at LT = 11.00, Ls = 168° (ORB1441_5). By means of an inverse radiative transfer code (Oliva et al., 2016) we retrieve the aerosols optical depth across the region and try to infer the connection between the local storm dynamics and the orography.

Instrument and data:

OMEGA (Observatoire pour la Minéralogie, l'Eau, les Glaces et l'Activité) is a visible and near-IR mapping spectrometer, operating in the spectral range 0.38-5.1 μm (Bibring et al., 2004). The instrument's IFOV is 1.2 mrad, corresponding to a spatial resolution of less than 350 m at periapsis. Three separate channels operate with different sampling to cover the whole spectral range. The first covers the range 0.38-1.05 μm and has a nominal spectral sampling of 7 nm; the second covers the range 0.93-2.73 μm with a spectral sampling of 13 nm; the third operates in the range 2.55-5.1 μm with a spectral sampling of 20 nm.

To study the local dust storm in Atlantis Chaos we have taken into account also observations cover-

ing the same region in which the storm is not present. The list of the considered observations is given in Table 1 and the corresponding reflectance factor spectra are shown in Figure 1.

Orbit	Lat [°]	Lon [°]	Ls [°]	$\tau_{9.3}$	Cl-i	res [km/px]
1441_5	-32.63	-176.51	168.62	0.18	0.92	4.27
1258_3	-32.64	-176.50	141.92	0.14	0.86	1.90
1474_5	-32.52	-176.43	173.69	0.23	0.67	4.76
3262_5	-32.62	-176.52	83.76	0.08	0.87	1.70
5161_3	-32.63	-176.51	14.53	0.11	0.93	0.86
5456_5	-32.62	-176.51	52.91	0.04	0.87	3.27

Table 1: list of the selected orbits covering the region of the local dust storm. Lat is the latitude, Lon is the longitude, Ls is the solar longitude, $\tau_{9.300}$ is the dust optical depth at 9.3 μm (Montabone et al., 2015), Cl-i is the cloud index and res is the spatial resolution. Latitude and longitude values are relative to the maximum optical depth region of the storm that has been imaged in orbit 1441_5.

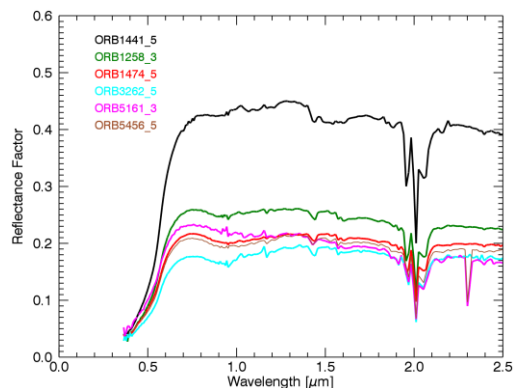


Figure 1: reflectance factor spectra of the selected observations, taken at the maximum optical depth region of the storm (see Table 1).

Method of the analysis:

To analyze the storm properties we have used the inverse radiative transfer model MITRA described by Oliva et al. (2016) to retrieve the effective radius r_{eff} , the optical depth at 880 nm τ_{880} and the top pressure tp of the dust layer. The temperature-pressure profile, the CO₂, CO and H₂O mixing ratios and the a-priori particles size distribution have been taken from the Mars Climate Database (MCD, Forget et al., 1999).

To perform the retrieval we have selected 5 observations of orbit 1441_5 spread up along the region where the dust cloud is present. All observations have been taken at longitude -176.5° and are separated by steps of 1° in latitude, from -32.6° to -

36.6°. At -32.6° the cloud presents its maximum optical depth. In this region the solar radiance is completely scattered by the dust and the underlying surface results to be hidden. However, moving southwards the optical depth decreases and the surface contribution cannot be neglected in the retrieval process.

Surface properties: Among the selected observations (see Table 1), we have verified that orbit 3262_5 is particularly suitable to analyze the region in almost clear sky conditions since water ice clouds are not present and the dust opacity, as retrieved by Montabone et al. (2015), is very low. A comparison of orbits 1441_5 and 3262_5 is shown in Figure 2.

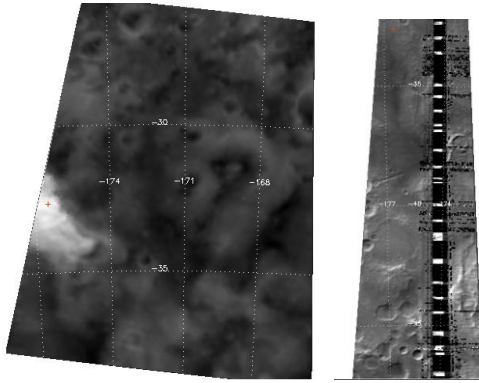


Figure 2: comparison between the regions covered by orbits 1441_5 and 3262_5, displayed at 1 μm . The red crosses indicate the regions where the reference spectra shown in Figure 1 have been taken.

To obtain the gas-free surface spectra of the studied region, we have processed the spectra of orbit 3262_5 using the SAS method (Geminale et al., 2015) that we briefly describe here. The method, based on the principal component analysis (PCA), searches for a set of eigenvectors whose linear combination is capable to reconstruct the measured spectrum (Bandfield et al., 2000). The physical significance to the eigenvectors matrix is given by best fitting a linear combination of the meaningful eigenvectors with a set of test vectors (Hopke, 1989). In our case, these vectors are simulations obtained with the radiative transfer code ARS (Ignatiev et al., 2005), each one representing a gaseous spectral endmember for CO_2 , CO and H_2O . A test spectrum for the surface is obtained with the so called Mons Olympus' method (MO, Langevin et al., 2005). The resulting surface spectrum used as input in the MITRA model is shown in Figure 3.

Retrieval of the dust properties:

We used the MITRA model to retrieve the microphysical and geometrical properties of dust. Gaseous absorption cross sections have been computed using the HITRAN 2012 database (Rothman et al., 2013) and exploiting the routines of the ARS

radiative transfer package (Ignatiev et al., 2005).

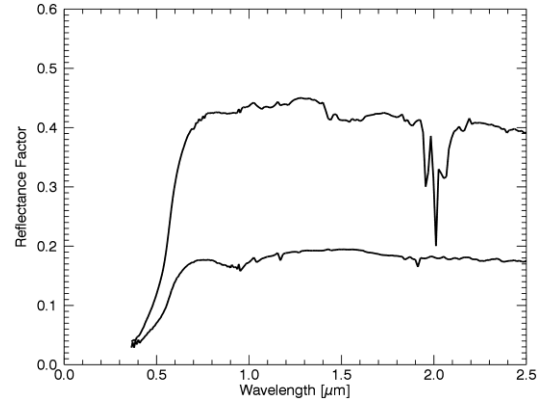


Figure 3: the lower spectrum is the retrieved surface reflectance at latitude = -33.6° and longitude = -176.5° of orbit 3262_5, obtained with the SAS method. The upper spectrum is the reflectance of orbit 1441_5 at the maximum optical depth region of the storm (red cross in the left panel of Figure 1).

To describe the optical properties of dust we considered the complex refractive index from Wolff et al. (2009). In the model we tested different scenarios to describe the vertical structure of the cloud, using more than one layer, different size distributions and refractive indices (e.g. Hansen, 2003). However, we verified that our first guess scenario consisting of a single layer described with the optical constants from Wolff et al. (2009) extending to the surface is able to reproduce the observed spectra in a reliable way, ruling out the requirement for more complex scenarios. We used the reflectance spectra obtained with the SAS method, as described in the previous section, as surface albedo spectra in input to the model. We then applied the model to retrieve the dust r_{eff} , τ_{880} and tp on all the selected observations. All retrievals have been performed in the spectral range 500 ÷ 2500 nm.

LT	-32.6°	-33.6°	-34.6°	-35.6°	-36.6°
r_{eff} [μm]	1.23 (0.21)	1.38 (0.02)	1.15 (0.12)	1.06 (0.07)	1.04 (0.08)
tp [mbar]	3.4 (0.3)	3.4 (0.7)	3.4 (0.7)	5.1 (0.5)	5.1 (0.5)
tp [km]	4.4 (1.1)	4.4 (1.9)	4.4 (1.9)	0.44 (0.05)	0.44 (0.05)
τ_{880}	5.9 (2.2)	3.4 (1.8)	1.3 (0.7)	0.7 (0.2)	0.6 (0.2)

Table 2: best fit values obtained from the retrieval on each observation. Latitudes are given in the first row (LT) and the values in parenthesis are the errors of the retrieved parameters.

Discussion and future work:

As expected, we found a decreasing trend for the optical depth going towards southern latitudes (i.e. going away from storm, see Figure 2). Indeed, we found that the opacity at 880 nm decreases from about 6 at latitude -32.6° to less than 1 at latitude -36.6°. Even if less evident, we found a decreasing trend also for the layer top altitude, decreasing from

about 4 km to less than 1 km along the covered spatial region (see Table 2).

In the future we plan to extend the retrieval in order to map the dust optical depth throughout the whole storm region. Moreover, using different orbits we will track the evolution of the dust opacity with time by performing the retrieval on averaged areas of each observation in Table 1. With this analysis we will discuss the possible connection between the storm dynamics and the orography of the region, and we will try to understand the origin of such an event.

Acknowledgements:

This study has been performed within the UPWARDS project and funded in the context of the European Union's Horizon 2020 Programme (H2020-Compet-08-2014), grant agreement UPWARDS-633127.

References:

- Altieri, F. et al., 2007. OMEGA/PFS observations of a local dust storm on Mars. Seventh International Conference on Mars, July 9-13, 2007, Pasadena, California.
- Bandfield, J.L. et al., 2000. Spectral data set factor analysis and end-member recovery: Application to analysis of martian atmospheric particulates. *J. Geophys. Res.* 105 (E4), 9573–9588.
- Bibring, J-P. et al., 2004. OMEGA: Observatoire pour la Minéralogie, l'Eau, les Glaces et l'Activité. Mars Express: the scientific payload, Ed. by Andrew Wilson, scientific coordination: Agustin Chicarro. ESA SP-1240, Noordwijk, Netherlands: ESA Publications Division, ISBN 92-9092-556-6, 2004, p. 37 - 49.
- Forget, F. et al., 1999. Improved general circulation models of the Martian atmosphere from the surface to above 80 km. *Journal of Geophysical Research*, Volume 104, Issue E10, 24155-24176.
- Geminale, A. et al., 2015. Removal of atmospheric features in near infrared spectra by means of principal components analysis and target transformation on Mars: I. Method. *Icarus* 253, 51-65.
- Gierasch, P.J. and Goody, R.M., 1968. A study of the thermal and dynamical structure of the Martian lower atmosphere. *Planet. Space Sci.* 16, 615–646.
- Hansen, G.B., 2003. Infrared Optical Constants of Martian Dust Derived from Martian Spectra. Sixth International Conference on Mars, July 20-25 2003, Pasadena, California.
- Hopke, P.K., 1989. Target transformation factor analysis. *Chemometrics Intell. Lab. Syst.* 6, 7–19.
- Ignatiev, N.I. et al., 2005. Planetary Fourier spectrometer data analysis: Fast radiative transfer models. *Planet. Space Sci.* 53 (10), 1035–1042.
- Kahre, M.A. et al., 2008. Investigations of the variability of dust particle sizes in the martian atmosphere using the NASA Ames General Circulation Model. *Icarus* 195, 576-597.
- Korablev, O. et al., 2005. Optical properties of dust and the opacity of the Martian atmosphere. *Advances in Space Research* 35, 21-30.
- Langevin, Y. et al., 2005. Sulfates in the north polar region of Mars detected by OMEGA/Mars Express. *Science* 307 (5715), 1584–1586.
- Määttänen, A. et al., 2009. A study of the properties of a local dust storm with Mars Express OMEGA and PFS data. *Icarus* 201, 504-516.
- Montabone, L. et al., 2015. Eight-year climatology of dust optical depth on Mars. *Icarus* 251, 65-95.
- Oliva, F. et al., 2016. Clouds and hazes vertical structure of a Saturn's giant vortex from Cassini/VIMS-V data analysis. *Icarus* 278, 215-237.
- Wolff, M.J. et al., 2009. Wavelength dependence of dust aerosol single scattering albedo as observed by the Compact Reconnaissance Imaging Spectrometer. *Journal of Geophysical Research*, Vol. 114, E00D04.